

# ARCES: an echelle spectrograph for the Astrophysical Research Consortium (ARC) 3.5m telescope

Shu-i Wang<sup>\*a</sup>, Roger H. Hildebrand<sup>\*\*b, c, d</sup>, Lewis M. Hobbs<sup>b</sup>, Stephen J. Heimsath<sup>a</sup>, Gary A. Kelderhouse<sup>a</sup>, Robert F. Loewenstein<sup>b</sup>, Solly Lucero<sup>c</sup>, Constance M. Rockosi<sup>b, e</sup>, Dale B. Sandford<sup>a</sup>, Jeffrey L. Sundwall<sup>a</sup>, Julie A. Thorburn<sup>a</sup>, Donald G. York<sup>b, c</sup>

<sup>a</sup>University of Chicago Engineering Center; <sup>b</sup>Department of Astronomy and Astrophysics, The University of Chicago; <sup>c</sup>Enrico Fermi Institute, The University of Chicago; <sup>d</sup>Department of Physics, The University of Chicago; <sup>e</sup>Department of Astronomy, The University of Washington

## ABSTRACT

A new echelle spectrograph was commissioned in 1999 for the ARC 3.5 meter telescope. The key features of the instrument are that it has a resolution of 9 km/sec, limited by the pixel size of the CCD; has no moving parts behind the slit during observation; provides complete spectral coverage from 3200Å to 10000Å, limited by the prism cross disperser material on the blue side and by the CCD sensitivity on the red side; provides blazeless spectra; achieves S/N>3000; and is remotely operable. The instrument is being used for studies of abundances in stars and for a large survey of diffuse interstellar bands.

## 1. OVERVIEW

The ARC Echelle Spectrograph, ARCES, is a high-resolution echelle spectrograph designed as a facility instrument for the Apache Point Observatory (APO) 3.5m Telescope. (APO is owned and operated by the Astrophysical Research Consortium, ARC.) The spectrograph covers a wavelength range of 320-1000 nm in a single exposure. The spectrum is recorded in about 130 echelle orders. The separation between orders ranges from about 9" (9 arc-seconds) in the blue, to 5" in the near IR. The method of dispersion is an echelle grating, which is combined with double-prism cross-dispersion in an in-plane arrangement. The large echelle grating is fed with a 200mm diameter beam from the f/10 telescope and a matching, off-axis, paraboloidal (OAP) collimator, which, when used with the f/2.7 Schmidt camera, permits a wide entrance slit of 1.6" on the sky. With reasonable seeing and careful focusing, ARCES should have minimal light lost at the slit. The two, very large, UBK7 prisms give relatively uniform spacing of the echelle orders and high throughput. The resolution is about 9 km/sec using a SITE Tk2048E, 2048x2048 CCD array detector with 24 µm pixels. The spectrograph characteristics are shown in Table 1. ARCES was commissioned in 1999<sup>1</sup>. Since commissioning, ARCES has enabled the observations of many scientific programs. Examples of the spectra may be seen in Snow et.al.<sup>2</sup>.

## 2. OPTICS

ARCES is located at the f/10 Nasmyth 1 port of the ARC 3.5-m telescope. The main spectrograph optics consist of an off-axis paraboloidal (OAP) collimator, an echelle grating, and two cross-dispersing prisms, located in the rough-vacuum upper tank, and an f/2.7 Schmidt camera with achromatic correctors, located in the low-vacuum camera tank/cryostat. Figure 1 shows the layout of the spectrograph optics. Light from the telescope enters through the spectrograph aperture into the upper tank, and a 45° mirror folds the beam onto the OAP collimator. The collimator reflects a collimated beam of 200mm diameter to the echelle grating, oriented in a conventional in-plane mounting. Two UBK7 prisms with 45° apex angles are mounted at the "elbow" of the upper tank to separate the echelle orders. The blue cutoff of the system sensitivity is primarily determined by the UV transmission of these prisms. The top view of

---

\* Current Affiliation: [swang@fltvis.com](mailto:swang@fltvis.com); phone 1 630 466-4343; fax 1 630 466-4358; <http://home.fnal.gov/~swang/>; Flight Systems, Inc., 43W752 Route 30, Sugar Grove, IL 60554-0250

\*\* [roger@oddjob.uchicago.edu](mailto:roger@oddjob.uchicago.edu); phone 1 773 702-7581; fax 1 773 702-8212; University of Chicago, Department of Astronomy and Astrophysics, 5640 South Ellis Avenue, Chicago IL 60637

Table 1. ARCES system specification.

<b>SYSTEM</b>	
Spectral Range	320 - 1000 nm
Resolving Power	33,000 with 1.6" slit, 24 $\mu\text{m}$ pixels, or a velocity resolution = 9 km/s
Sensitivity	$V = 16$ yields 0.2 count/resolution element/sec
Entrance Aperture	1.6"x1.6" or 1.6"x3.2", manual change
Platform	ARC 3.5m Telescope Nasmyth Port without Focal Plane Rotator
Cooling Scheme	LN2 with autofiller
Volume	
Upper Tank	970 liters
Camera Tank	210 liters
Weight	
Upper Tank	900 lbs
Camera Tank	700 lbs
<b>SUBSYSTEMS</b>	
<b>TELESCOPE</b>	
Type	Ritchey-Chretien
Aperture	3.5 m
Focal Ratio	f/10
Platescale	5.86 arcsec/mm
<b>CALIBRATION</b>	
Calibration lamps	Thorium Argon (Th-Ar) hollow cathode lamp, Quartz Tungsten Halogen (QTH) lamp
<b>GUIDE CAMERA</b>	
Camera System	Photometrics SenSys 1600 Camera
Detector	KAF 1600, 1536x1024 array with 9x9 $\mu\text{m}$ pixels
Platescale	0.05 arcsec/pixel, normally binned 3x3 yielding 0.151 arcsec/bin pixel
FOV	1.35 arcmin x 0.9 arcmin
Operator Options	Manual, auto guide, auto trail
<b>SPECTROGRAPH</b>	
Magnification	0.27x
Final Platescale	21.8 arcsec/mm = 0.52 arcsec/pixel, perpendicular to the dispersion
Collimator	f=2,032 mm, D=225mm (200mm beam size), f/9 Off-axis Parabola, quartz substrate
Echelle Grating	B&L, 204mm x 408mm, 31.6 grooves/mm, 64.6° blaze angle, 69.5° incident angle
Cross-disperser	two 45° UBK7 Prisms, minimum deviation; total deviation through both = 52.7°
Camera	Schmidt type with LLF2 (12.7mm thick) + UBK7 (19.05mm thick) doublet corrector
Schmidt mirror	f=540mm, D=381mm, f/1.4 Zerodur mirror
Field Flatteners	UBK7 Plano-convex lens, f=839mm, D=75mm (matched to CCD curvature)
Detector	
Type	SITe TK2048E back illuminated 2048x2048 CCD with 24 $\mu\text{m}$ x 24 $\mu\text{m}$ pixels
Operating Temperature	160K (-110C)
Read Noise	7 e-
Dark Current	7.35 e-/pixel/hour
Full well	150,000 to 200,000 e-
Gain	3.8 e-/DN
Nominal curvature	1581 mm, convex @ 300K; 1535 mm convex @ 160K with stiffener

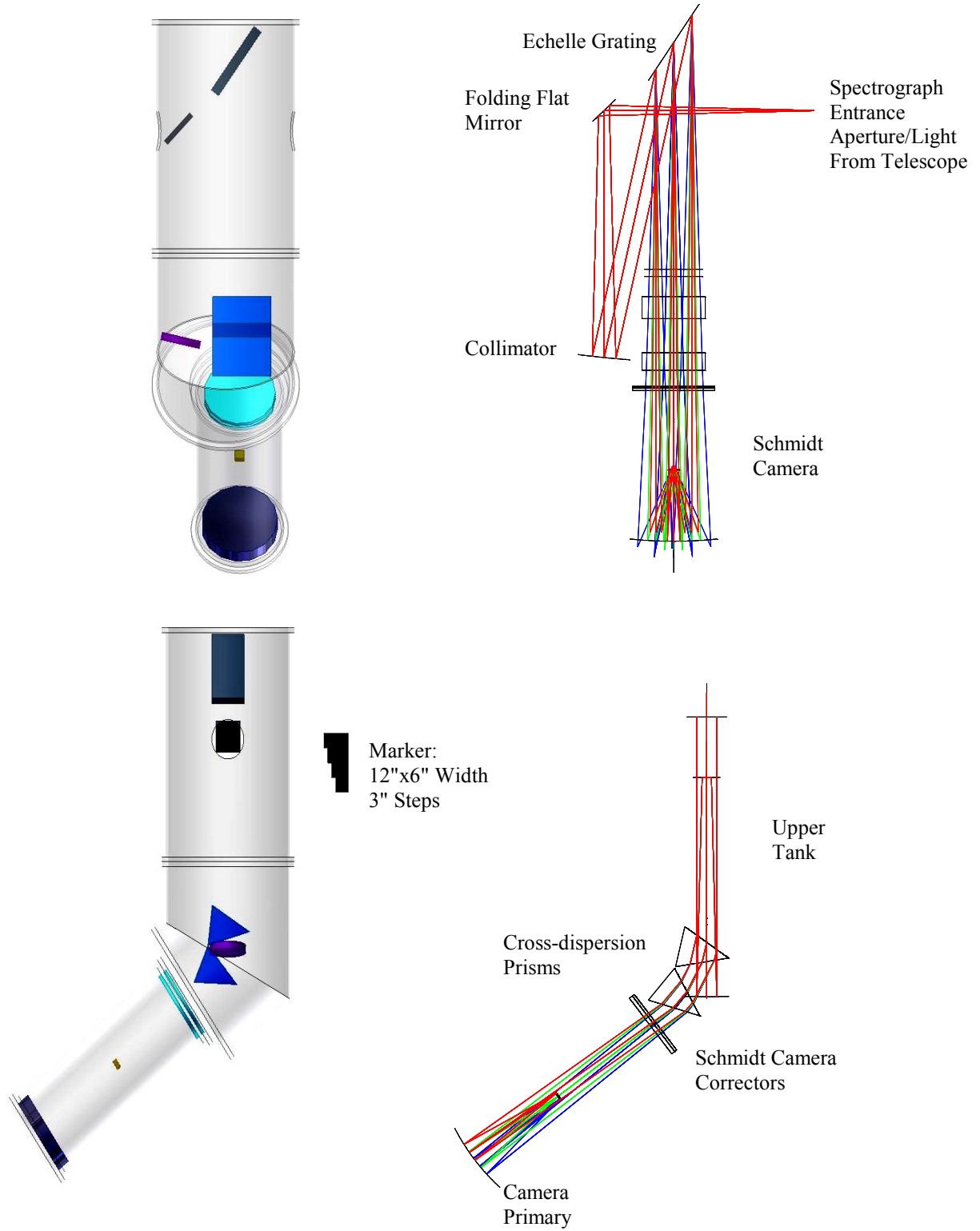


Figure 1. ARCES mechanical layout on left, and raytrace on right.

Figure 1 is a projection in the plane of the echelle dispersion, and the bottom view is in the plane of the cross-dispersion. The Schmidt camera tank is mounted to the elbow, or spherical joint, of the upper tank. The spherical joint allows rough adjustment of the cross-dispersed orders on the CCD. The Schmidt corrector design is an airspaced doublet configuration consisting of a LLF2 aspheric plate and an UBK7 aspheric plate with their plane sides facing each other. The corrector plates double as the vacuum window for the Schmidt camera. The f/2 spherical camera mirror reflects the light to a SITe Tk2048E 2048x2048 CCD array with 24  $\mu\text{m}$  pixels located about halfway between the corrector plates and the camera mirror. The spectrograph should also work well with a 2048x4096 pixel format CCD with 15  $\mu\text{m}$  pixels. The SITe CCD has a room temperature bow of about 1581mm convex curvature<sup>3</sup>. To reduce and control the change in the bowing of the CCD upon cooling, a kovar stiffener plate is attached to the back of the CCD. The bow becomes more convex by about 10  $\mu\text{m}$  when the CCD and stiffener are cold, giving us a cold radius of 1535mm. A field flattener lens is mounted in front of the CCD to match the curved field.

The mirrors in the upper tank and the Schmidt camera mirror were coated with a bare aluminum coating. The fused silica entrance window for the upper tank and the UBK7 CCD field flattener have been coated with a wide-band AR coating by QSP Optical Technology Inc. (Santa Ana, CA). The AR coating has an average reflectivity of 1% over the 320 – 1100nm spectral range, with a maximum reflectivity of 3%, and a maximum absorption of 0.5%.

The spectrograph optics have been described in detail by Schroeder<sup>4</sup>. The current system differs in that a small "wedge" prism, used in the original design, no longer exists. The prism was inserted in different apex positions to shift the orders perpendicular to the dispersion on an 800x800, 15  $\mu\text{m}$  pixel CCD. The motion of the grating was originally needed to shift the long, red orders parallel to the dispersion, but has now been disabled. The 800x800 CCD has since been replaced by a larger CCD.

### 3. MECHANICS

#### 3.1 Mechanical Layout

The spectrograph is mechanically separated into 2 sections: the upper tank contains the collimator and dispersing elements in a low vacuum (200 milliTorr, for thermal and pressure stability and cleanliness), and the camera tank contains the camera optics and detector cryostat components in a high vacuum. The camera tank is the enclosure and mounting structure for the Schmidt camera optics. The entire 210 liters volume of the tank also functions as the cryostat for the CCD, and so contains the liquid nitrogen reservoirs for cooling the detector and a cold shield, as well as the CCD preamplifier and clock voltage conditioning electronics. The CCD is mounted at the focus of the Schmidt Camera, not kept in a separate dewar. This setup permits faster camera optics but makes access to the CCD a time consuming process. An enclosed front-end is attached to the entrance port of the spectrograph upper tank. The front-end contains the spectrograph aperture, guide camera, and calibration subassemblies. Section 5 details the front-end elements.

The overall design makes the spectrograph extremely stable. The stationary Nasmyth telescope mount, with kinematic x, y and tip/tilt adjustments, eliminates flexure with on-sky positions. A "foot" support under the camera tank located at its center of gravity further enhances stability. The CCD is held fixed with respect to the Schmidt mirror with an invar frame, so the camera focus is not subject to short-term drifts. The location of the star/object and quartz calibration orders drift through the night by 0.5 pixels over 10 hours, but return to the same position the next night. The drift is most likely due to the thermal changes of the prisms with temperature. The stability in the grating dispersion direction is excellent. The shift is systematic through the night and amounts to 0.35 pixels in 10 hours, or 0.18 pixels (0.7 km/sec) per 5 hours. While this drift is twice our design goal of 0.1 pixels in 5 hours, it occurs mostly in the first half of the night. In the second half of the night, the drift is less than 0.3 km/sec/5 hours. As a practical matter, a 5 hour exposure would not be taken on a bright source, and the drifts in the first half can be easily calibrated out by interpolating between calibrations made every hour. In the second half of the night, even a 5 hour integration could be done.

#### 3.2 Camera Cryostat

The function of the cryogenic system for the ARCES camera is to hold the CCD at its operating temperature of 160K; the rest of the optical and mechanical components in the tank remain at room temperature. The detector is cooled by

attaching the CCD package to a copper block, which is connected through copper cold straps to a liquid nitrogen reservoir in the camera tank. The operating temperature of the detector is then regulated to better than 1° by controlling the current in a 40Ω resistor in the cold block. The CCD is mechanically mounted in a Kel-F fixture, which is in turn suspended at the focus of the Schmidt camera by a 4-vaned spider assembly; the vanes for the spider were made out of a glass filled polyimide (Kapton) sheet. The low thermal conductivity of Kel-F and small physical cross-section of the spider vanes and mounting fixture where it touches the cold CCD package thermally isolates the 160K CCD from the rest of the room-temperature camera tank. The spider vanes are mounted to two concentric rings for remote CCD tip/tilt adjustments. The rings are mounted to the camera mirror assembly via two precision screws that allow remote CCD focus adjustments. The maximum obscuration ratio of the Schmidt camera as a result of the size of the CCD mount and the CCD tip/tilt/focus assembly is 0.2.

Table 2 shows the factors involved in controlling the CCD temperature. The dimensions of the cold straps are chosen so that a heater input of ~ 2.5 watts (in addition to radiation from the room temperature walls of the cryostat) is sufficient to balance the heat flow through the cold straps to the LN2 reservoir when the CCD is at the operating temperature. The joints in the cold straps are constructed of thin copper and silver straps folded in such a way as to permit nearly torque-free tip, tilt, and focus adjustments to the CCD. Two screw joints must be disconnected whenever the CCD block is removed. Cryogenic-application grease mixed with aluminum nitride powder is used at the joints to ensure good thermal contact.

Table 2. Temperature control.

Acceptable operating range for CCD	160K ± 10K
Equilibrium CCD temperature (no regulating current)	136K
Temperature variations (regulated)	< 0.1K
Power into control heater	~ 2.5 watts
CCD Cold Straps Parallel straps one silver, 0.010" X 2" X 6" two high-purity oxygen-free copper, 0.005" X 2" X 6" Each strap in two sections: one 4" & one 2"	

In principle, the cryogenic system would require no other components. In practice, as explained in the next paragraph, the large room-temperature interior surface area of the camera tank surrounding the cold CCD necessitates a second LN2 reservoir and an ion pump to overcome the effects of outgassing. The interior surface area of the camera tank is ~ 2 square meters and must be kept at room temperature because of the camera tank's structural role in supporting the Schmidt camera optics. We have found that despite adsorptive pumping by charcoal getters and efforts at the use of good vacuum practice, outgassing from this large interior surface area will slowly freeze out on the cold surfaces. The first indication of frosting is an increase in the unregulated equilibrium temperature of the CCD due to a decrease in the emissivity. On careful inspection frost became visible on all cold surfaces after a day or two.

The solution to this dilemma that we settled on was to place an ion pump in the camera tank that pumps continuously on the tank while the CCD is cold. We also added a second LN2 reservoir of larger capacity, to cool a gold-plated, copper, cold shield and a plate of charcoal getter mounted to the reservoir. The getter consists of a 0.06" oxygen-free, copper plate of 10" diameter. The entire getter surface is covered with coconut charcoal (Calgon) epoxied on with Eccobond 286. The cold shield sits inside the camera just outside the beam path to trap stray gas molecules. This shield is colder and much larger (~ 0.14 square meter per side) than the CCD and is cooled for at least two hours before filling the CCD LN2 reservoir. The two reservoirs are sized so that if the LN2 supply is cut off, the CCD reservoir empties first and the reservoir that cools the shield and getter will stay full long enough that the detector is at or near room temperature before the getter warms up and releases its accumulated gas into the tank. Table 3 shows procedures for the cooling and warming cycles such that no frost forms on the CCD. A sensor system is in place to alert the local staff in case an unscheduled warm up of the CCD occurs, so the status of the two reservoirs can be checked and monitored.

The LN2 reservoirs are automatically refilled every 4 hours with an autofill system<sup>3</sup> which connects the reservoirs to an LN2 transfer dewar via vacuum-jacketed lines. The transfer dewar is an 80-liter, Cryofab dewar, which is refilled about

every two days by the observatory daystaff. Automatic refills of the reservoirs while observing do not adversely effect the wavelength stability of the instrument.

Table 3. Cooling and warming cycles.

Cool Down Procedure	Pressure	Time
1. Start pump (16 cfm dry scroll pump; 300 l/s turbo pump).	1 atm $\rightarrow$ $5 \times 10^{-5}$ torr	$\sim$ 12 hrs
2. Leak check dewar.		
3. Fill shield reservoir <sup>a</sup> .	$5 \times 10^{-5}$ torr $\rightarrow$ $5 \times 10^{-7}$ torr	
4. Start ion pump (300 l/s diode type ion pump).	$5 \times 10^{-6}$ torr $\rightarrow$ $1 \times 10^{-7}$ torr	
5. fill CCD reservoir <sup>b</sup> . Read out CCD while cooling to keep thermally generated electrons from freezing into traps.	$1 \times 10^{-7}$ torr $\rightarrow$ $< 1 \times 10^{-7}$ torr	2 – 3 hrs after step 3
6. Reach CCD operating temperature.	$1 \times 10^{-7}$ torr	2 – 3 hrs after step 5
7. Enable the autofill system to automatically refill reservoirs.		
<b>Warm up Procedures</b>		
1. Let CCD reservoir go empty and let CCD warm up to 0C, keeping shield reservoir cold <sup>c</sup> .		$\leq$ 8 hrs
2. Turn off ion pump.		
3. Let shield reservoir go empty <sup>c</sup> .		
4. Let shield and shield reservoir warm up.		$\sim$ 12 hrs

<sup>a</sup>Shield reservoir: capacity = 15 liters; hold time = 22.5 hrs. A coconut charcoal getter is in thermal contact with bottom of shield reservoir.

<sup>b</sup>CCD reservoir: capacity = 3 liters; hold time = 8 hrs.

<sup>c</sup>Because shield reservoir has larger capacity, it will automatically stay cold for  $>$  14 hrs after the CCD reservoir is empty. Process can be speeded up by backfilling the camera tank with dry nitrogen.

#### 4. DATA AND ELECTRONICS

The CCD electronics are slightly-modified versions of the camera electronics for the Sloan Digital Sky Survey (SDSS) Photometric Camera<sup>3</sup>. The conceptual layout for the electronics is shown in Figure 2. A Macintosh computer functioning as the Instrument Control Computer (ICC) resides inside the observatory computer room. It communicates with the CCD controller saddlebag and the Motor Control Computer (MCC) via fiber links. The saddlebag, mounted to the camera tank, contains an analog circuit board, which provides the CCD voltages and does the temperature regulation, processing and digitization of the pixel data, and a Forth microcontroller which communicates with the ICC. The Forth microcontroller provides the CCD clocking signals and runs the autofill system. Attached to the saddlebag is another box which contains the fiber converters for the CCD data and the shutter controller. The MCC resides at an intermediate level rack in the telescope dome, along with the UPS and calibration lamp power supplies. The MCC controls the motor driver electronics located in a Pit Rack next to the spectrograph camera. Motorized parts include the CCD tip/tilt/focus, filters for the guide camera and calibration lamps, the calibration flip mirror, and the spectrograph aperture focus. Only the calibration flip mirror and the calibration filters are used routinely. A separate Macintosh computer resides inside the computer room for controlling the guide camera. It communicates with the guide camera with a fiber SCSI link. The ARCES ICC is connected to the Observatory Control Computer, which passes commands and status information between the instruments and the remote observing stations<sup>5</sup>. Details of the software user interface and helpful hints for observing with the Echelle spectrograph can be found at: <http://astro.uchicago.edu/echelle/>.

#### 5. ECHELLE SPECTROGRAPH FRONT-END

##### 5.1 Overview

The Echelle Front-end is a box located between the telescope port and the Echelle Spectrograph Upper Tank. The Front-end attaches to the Upper Tank entrance window assembly, and holds the spectrograph aperture, guide camera and calibration optics subassemblies. The subassemblies are mounted on a focus slide such that the subassemblies can be moved along the telescope optical axis as a unit. This arrangement allows focusing of the aperture during alignment.

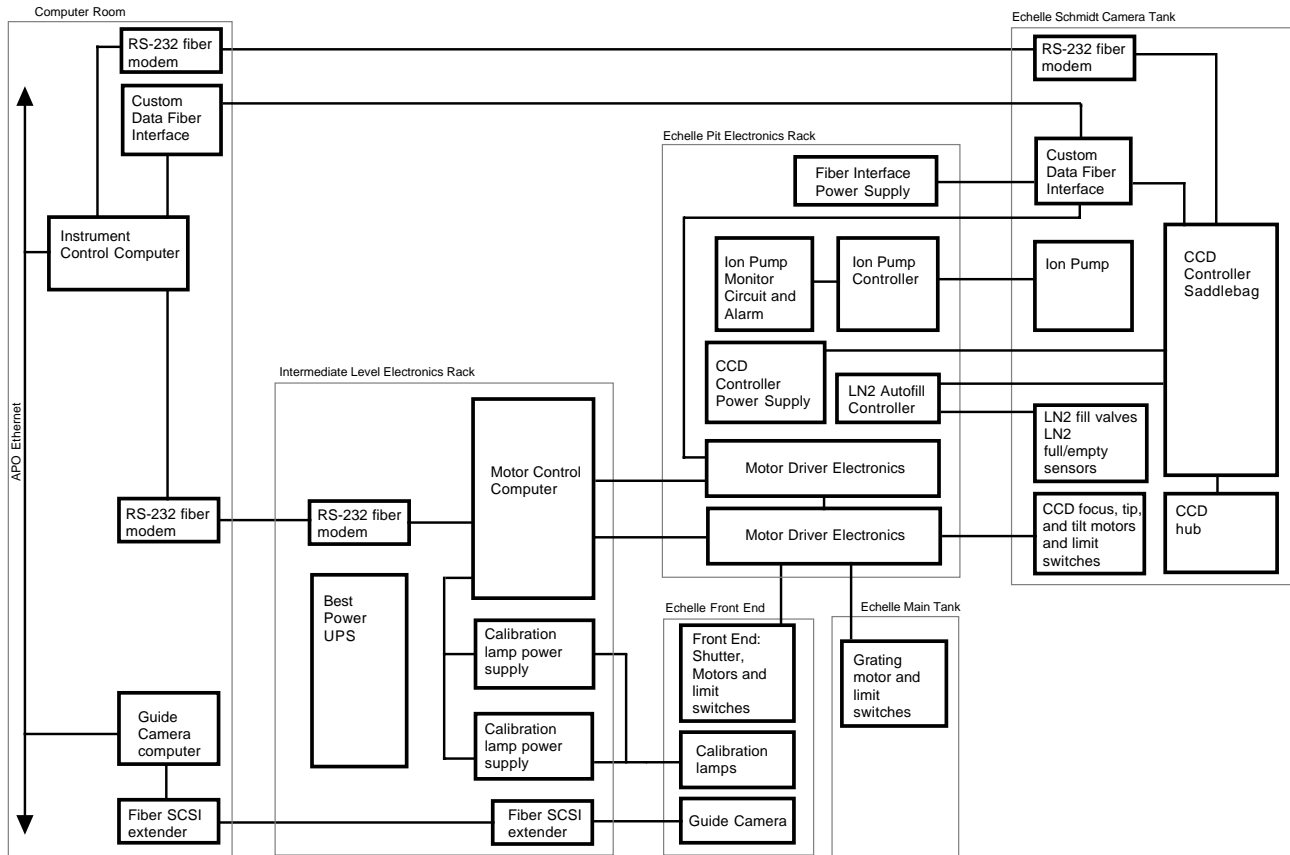


Figure 2. Echelle electronics layout.

## 5.2 Spectrograph Aperture

The spectrograph aperture is mounted on a light-tight fixture located in the middle of the front-end focus slide. The front side of the aperture box holds the spectrograph entrance aperture. A baffle made of a large bellows extends from the back of the aperture box to the shutter. The shutter is mounted on the entrance window port of the upper tank. Two apertures are available: 1.6"x1.6", 1.6"x3.2". The larger aperture is normally preferred, as it does not limit operations in good seeing and it allows more light through when seeing is poor. Switching between apertures is a manual operation. Each aperture is mounted in an aperture holder assembly which mounts to the aperture box with 2 screws. Alignment pins on the aperture box are used to align the aperture holder assembly with respect to the spectrograph dispersion axes.

## 5.3 Guider

The spectrograph aperture is made from a reflecting substrate. The aperture is tilted at an angle of 15 degrees. A fold mirror sends light reflected from the spectrograph aperture onto a slit viewer camera subassembly. A Nikon camera lens (105mm, f/2.8) is used to relay a 1:1 image of the aperture onto the CCD camera. A 6-position filter wheel is located at the pupil image plane between the lens and the camera. The six filters currently installed in the filter wheel are ND 0.04 (equivalent to open position, filter used for path length compensation), ND 1, ND 2, ND 3, red (Schott RG665, 2mm thick), and blue (Schott BG12 (1mm) + BG39 (1mm)).

The current guide camera is a Photometrics (Roper Scientific) SenSys 1600 Camera. The camera uses a KAF 1600, 1536x1024 CCD with 9x9 $\mu$ m pixels. The field of view (FOV) of the CCD is 1.35 arcmin x 0.9 arcmin. The apertures

are on 1.24 arcmin diameter substrates. The slit viewer camera sees a FOV larger than the reflective aperture substrate in the prism dispersion direction, and a FOV smaller than the substrate in the grating dispersion direction. During "normal" operation, the CCD camera is usually binned 3x3 to give 0.15"x0.15" pixels. The guider CCD is free of dead areas. However, the CCD is only cooled to +10C, and the guider is therefore limited by hot pixels and dark current to viewing a 15th magnitude object without dark subtraction. With dark subtraction of an image of the same integration time (a software option used with faint objects), the guider can view the wings of a 16th to 17th magnitude object on the slit with a two-minute integration. We plan to replace the Guide Camera with a cooled unit during the year 2002.

The user interface (REMARK) allows the operator to guide manually, in 0.1 arcsecond minimum steps; to use an autoguider that uses the reflected light from the aperture substrate to implement a quadrant balance of the wings of the image of the guide star; and to auto trail along the long dimensions of the aperture.

#### 5.4 Calibration

Two calibration lamps are available: a quartz-tungsten-halogen (QTH) "white" lamp and a thorium-argon hollow cathode lamp. The lamps are mounted to a 2" integrating sphere located on the spectrograph front-end. The integrating sphere has three 0.5" input ports, and a 0.5" exit port. Light exiting the integrating sphere is transmitted through an aperture stop with a central obscuration to simulate the f/10 beam from the telescope. An achromatic doublet images the exit port of the integrating sphere onto the spectrograph aperture, and forms a virtual image of the aperture stop of about the same size and distance as the telescope pupil. A fold mirror is flipped into the beam path during calibration to direct the calibration beam onto the spectrograph aperture. The fold mirror is flipped out of the beam path during telescope observations. This mirror and the two filter wheels are the only moving parts used during normal operations. Aperture focus, collimator focus, and CCD focus are checked, but have not required any changes for three years.

The QTH lamp has a 6-position filter wheel between the lamp assembly and the integrating sphere. Position 2 of the filter wheel currently has a blue filter identical to the guide camera blue filter (Schott BG12 (1mm) + BG39 (1mm)). The blue filter is useful for obtaining the blue end of the spectrum since the red end tends to saturate the spectrum, unless it is attenuated by the noted filter combination.

### 6. DATA ANALYSIS

The ARCES is capable of complete wavelength coverage from 3200Å to 10,000Å in 130 spectral orders. A typical extraction includes about 107 orders. Shorter wavelengths can be observed in very blue objects. Figure 3 shows plots of an ARCES spectrum of HD 183143. HD 183143 is a B7Ib star with  $E(B-V) = 1.4$  and  $V=6.2$ . Interstellar atomic and molecular lines, diffuse interstellar bands, stellar lines, and telluric absorption lines are visible in the spectrum. Note the strong diffuse bands at  $\lambda = 4430 \text{ \AA}$ ,  $5780 \text{ \AA}$ , and  $6284 \text{ \AA}$ .

Due to the exceptional number of recorded orders and the relatively large size of the detector pixels, the ARCES poses a data reduction challenge for standard data reduction packages. Reduction of ARCES data is performed using the echelle package in the National Optical Astronomy Observatory's (NOAO) Image Reduction and Analysis Facility (IRAF). Because certain ARCES data characteristics vary significantly from a typical echelle spectrograph, data reduction procedures are slightly modified from the conventional methods. Aliasing is easily introduced by IRAF routines, which do not perform fractional pixel weighting. A paper detailing the data reduction techniques is in preparation<sup>6</sup>. A data reduction guide to aide the user in using IRAF routines to extract maximum information from ARCES data can be found at: [http://www.apo.nmsu.edu/Instruments/echelle/ARCES\\_data\\_guide.pdf](http://www.apo.nmsu.edu/Instruments/echelle/ARCES_data_guide.pdf).

Flat fielding in particular requires different methods than are most often used in IRAF. The first difficulty arises from limited slit length in the ARCES, which causes QTH lamp orders to be approximately the same width as those in a typical object exposure. Forming a two-dimensional quotient of two similar width orders leads to improperly weighted sums and noise amplification unless aperture mask profiles are independently imposed upon the data. For this reason, two-dimensional flat fielding is not recommended for ARCES. More detrimental to the data integrity however are the problems inherent in dividing one narrow order by another: the aliasing present in a narrow-order ARCES exposure (discussed below) is greatly increased in severity when a quotient is formed. To avoid these difficulties and in lieu of



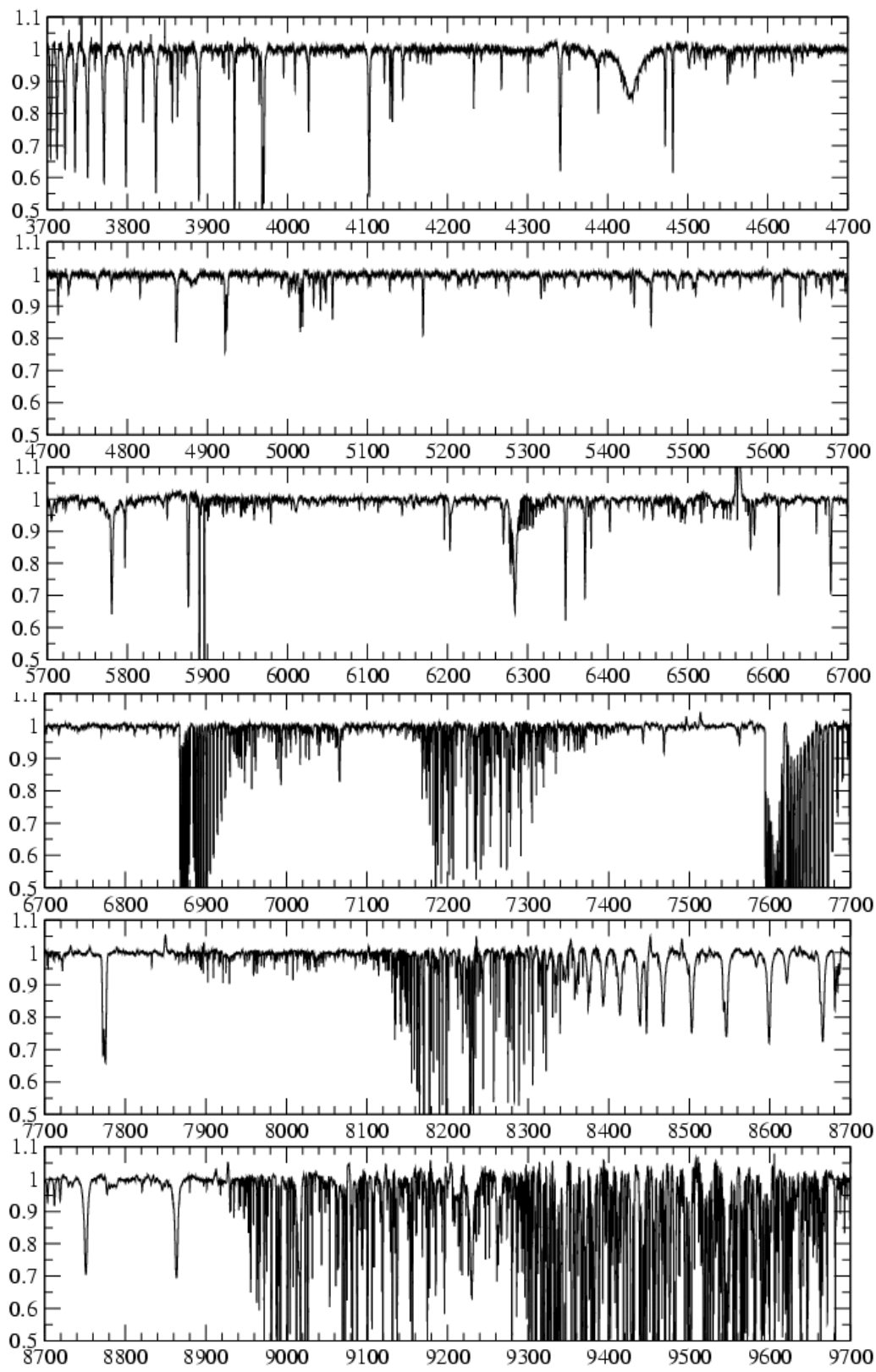


Figure 3. ARCES Spectrum of HD 183143 from 3700Å to 9700 Å, assembled with 93 echelle orders.

two-dimensional flat fields, one-dimensional flat fielding is performed after spectral extraction and before assignment of a dispersion function. This technique permits signal-to-noise ratios of up to 3000 in summed ARCES data.

ARCES data extraction itself is complicated by mild aliasing in the prism dispersion direction. Originally designed for a detector for smaller pixels, the ARCES has narrow (full width at half maximum  $\sim 3$  pixels) and closely spaced orders which, as is the case in all echelle spectrographs, do not run perpendicular to the isowavelength contours, or the grooves of the echelle grating. Prismatic cross-dispersion further exacerbates aliasing in minimally sampled ARCES data by introducing order curvature which varies as  $\lambda^{-3}$ . If ARCES data are extracted in the conventional manner without special measures to minimize the effects of aliasing, particularly in high-signal data, a semi-regular "ripple" pattern is observed in the extracted spectra. Similar effects are well documented in other instruments with minimally sampled spectral orders (e.g. the Space Telescope Imaging Spectrograph (STIS) as documented in Leitherer, C., et al. 2001, "STIS Instrument Handbook", Volume 5.1, (Baltimore: STScI)). Noise due to undersampling is reduced in STIS by dithering the source light along the length of the entrance aperture. Similarly, ARCES observers pursuing high signal-to-noise spectra are encouraged to trail objects along the slit length when possible. Despite these precautions, generic echelle spectral extraction using the 'apall' task in IRAF will cause aliasing ripples of moderate amplitude ( $\sim 0.8\%$ ) and low, slowly varying frequency to appear in extracted orders. Although 'apall' does include provisions for fractional pixel weighting in the wings of aperture masks, it does not do so in areas of high signal and thus does not retrieve maximum information from ARCES data.

To minimize the deleterious effects of line spread function undersampling, individual ARCES object spectra are increased in scale by a factor of four in the prism dispersion direction: rather than 2048 pixels, spectra are linearly interpolated to 8192 pseudopixels in the reduction process. Aperture traces are then calculated in the conventional way and used as a guide for 'apscatter' to remove scattered and background light in the expanded scale images. Final spectral extraction is then performed on the interpolated, background subtracted data. A similar strategy is employed to convert summed QTH flat field exposures to a one-dimensional format. Extracted object spectra are then divided by the one-dimensional flat field and then normalized. Wavelength calibration is derived from two-dimensional Chebyshev polynomial fits to arc line positions in extracted thorium-argon lamp exposures. Typically, a fourth order fit in both the grating dispersion and prism dispersion directions is sufficient to remove residuals and leave rms scatter of 0.025 Å. After dispersion correction, individual echelle orders are weighted and summed in wavelength space to generate a single "blazeless" spectrum covering the entire spectral range of ARCES.

## 7. COMMISSIONING

ARCES was taken through a series of tests that constitute science commissioning during the first quarter of 1999. Several stars were observed with well known interstellar spectra. The data showed excellent agreement with observations using other instruments. The resolution, as measured by the FWHM of calibration lamp lines, is uniform over the field. For single line measurements, the FWHM is 2.2 pixels, with a  $2\sigma$  error of 0.16 pixels, over the entire spectrum. This performance translates to a spectral resolution of about 33,000, or a velocity resolution of 9 km/s. The wavelength scale of ARCES can be determined at any one time to very high precision, using the Th-Ar lamp or using the telluric lines near 700nm and the dispersion constants of the echelle. This last technique gives a scale with an accuracy of 0.1 pixel. The read noise for the CCD and the electronics was measured to be 7 electrons 1 sigma, with a gain setting of 3.8 electrons per data number. The dark current was measured to be 7.35 electrons per pixel per hour averaged over the CCD. This level of dark current, 0.002 electrons per second, or 29 electrons per pixel in 4 hours, contributes less than read noise for practical exposure times with ARCES. This value of dark counts seems to be high by a factor of 30 compared to lab results on the same device. Although the dark current is not a factor currently, it does have a dominant effect on projections of S/N ratios in future upgrades planned to allow observations of fainter objects with a lower read noise CCD. We plan on reworking the CCD cold straps in the future to run a new CCD colder.

We checked the spectrograph's ability to obtain absolute velocities by taking a few radial velocity standards at different positions in altitude and azimuth, ranging over the entire sky. One order near 496nm was cross correlated with a daytime sky spectrum, assumed to have 0 radial velocity. Corrections for the motion of the Earth and the Sun were made for each stellar spectrum obtained. Otherwise, no corrections were made. There is a 3.6 km/sec shift that is

systematic, but with that correction, the rms scatter from a linear regression is 1.1 km/sec. Similar results were obtained for the few other orders tried. For precise work, the zero point and the dispersion in data points can be improved upon.

Stray light and crosstalk may appear between the orders due to scattering out of the orders, ghosts from intensely illuminated parts of the chip, light generated internal to the spectrograph, or from light entering the spectrograph through light leaks. Various light leaks were found and plugged during commissioning, and we are not aware of any internal sources of light remaining within the spectrograph. Figure 4 is a stacked plot depicting two adjacent echelle orders in the vicinity of a strong telluric absorption complex. The nearby order shows no apparent sign of cross-contamination by its neighbor. The background subtraction scheme used functional fit to interorder light. The 2-d functions used to approximate the interorder light pattern are smoothly varying in the grating dispersion direction and they cannot introduce or remove high frequency events in this axis. This performance is further evidence that the actual crosstalk between orders is indeed very low.

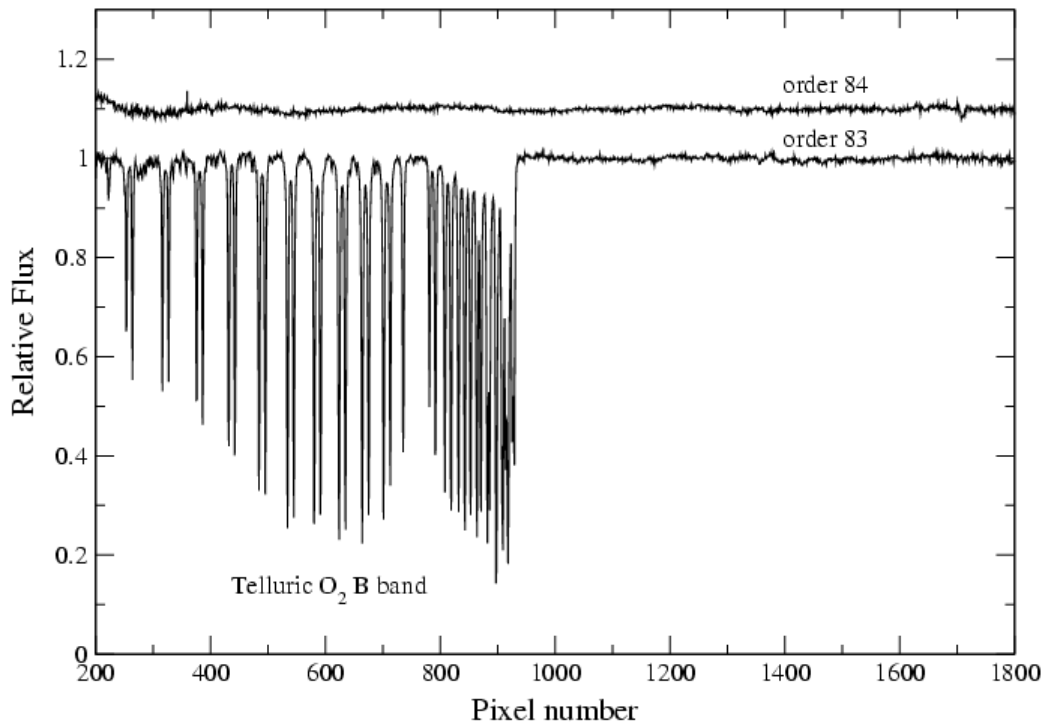


Figure 4. Stacked plot of HD 183143 depicting two adjacent echelle orders in the vicinity of a strong telluric absorption complex. The telluric lines in one order produce effects in the adjacent order of  $< 1.0 \text{ m\AA}$ ,  $5\sigma$ .

Cosmic rays appear as sharp, bright spikes in the ARCES data during long exposures. The number of pixels affected is about 1 in 75 in one hour. When binning  $2 \times 2$ , the number of affected pixels would be 1 in 20. This number of radiation hits reduces the advantage of binning for increasing the signal to noise ratio in long exposures. Clearly, for such long exposures, median filtering of multiple long exposures is sound practice for identifying cosmic rays. There does not seem to be an excess of radiation attributable to the echelle spectrograph itself (i.e., radioactivity from glass or metal.), because instruments using completely different configurations of CCDs at APO show the same relative effects. Cosmic rays provide the current limit on the length of exposure time. Replacing the current CCD with a CCD of smaller pixels would help, since most of the events affect only a single pixel.

About 2% of the photons entering the atmosphere for an APO echelle target reach the computer disk as data numbers on a good night. Estimates of the telescope efficiency alone suggest that the peak efficiency of the spectrograph is  $8\% \pm 2\%$ , against a goal of 9%. Exposure times can be estimated by assuming that a signal-to-noise ratio of 100 per resolution element (two pixels) is reached in one hours on a star of magnitude  $V=13$ , in good seeing with no trailing, for the region

of peak sensitivity (600 - 680 nm). The detected number of photons decreases continuously to the red and the blue of the peak, dropping by a factor of two by 820nm and 460nm, respectively, for an unreddened FO sub-dwarf.

The bright object limit is set by saturation of the CCD at the peak count rate (between 600 – 680 nm for most sources). Assuming a shortest exposure of 1 second, for practical reasons, a 0 magnitude object would just be observable on a good night, without saturating. The faint limit is set by the performance of the guider, the read noise of the chip, the rate of radiation hits and the mechanical stability of the spectrograph. In practice, because of the need to use short exposures to permit median filtering to remove cosmic rays, the limiting magnitude is  $V=15$ . With a guider that permits observing an 18<sup>th</sup> magnitude object and installation of a new CCD with 2 electrons read noise and negligible dark current, the limiting magnitude of 18 in 20 hours ( $S/N=10$ , per resolution element) would be set by photon noise.

## 8. CONCLUSION

ARCES has been shown to be a stable facility instrument enabling many science programs. The resolving power is limited to 33,000 by the large (24  $\mu\text{m}$ ) pixel size. Analysis indicates that with 15  $\mu\text{m}$  pixels, the resolving power would be limited at 54,000 by zonal errors on the aspheric corrector plates. The combined telescope/spectrograph system efficiency is  $>2.2\%$  at 647nm. With assumptions about the telescope mirror reflectivity, we estimate the spectrograph efficiency as  $8\pm 2\%$  at 630nm. The throughput can be further improved by applying wide-band anti-reflection (AR) coatings to the prisms and corrector plates. The spectrograph bright limit is 0 magnitude  $V$  at 630 nm. The radiation hits are 0.013 /pixel-hour, severely limiting the time length of a single exposure. The faint limit is 16.5  $V$ ,  $S/N > 20$  (the  $S/N$  refers to one resolution element, or two pixels) in 20 hours, limited by cosmic rays and the repeated read noise from  $\frac{1}{2}$  hour integrations. The faint limit can improve to 18<sup>th</sup> magnitude with a cooled guider sensor, and an improved CCD with lower read noise and with smaller pixels, to decrease the effects of cosmic rays. The CCD uniformity is good enough that no flat fielding is needed for  $S/N$  up to 500 at wavelengths less than 700nm. At longer wavelengths, fringing fluctuations may be as high as 20%. The spectrograph is mechanically stable to shifts of 0.2 pixel in wavelength per 5 hours. Only seasonal checks of the spectrograph internal focus are needed.

## 9. REFERENCES

1. Based on observations obtained with the Apache Point Observatory 3.5-meter telescope, which is owned and operated by the Astrophysical Research Consortium.
2. T. P. Snow, D. E. Welty, J. Thorburn, L. M. Hobbs, T. Oka, B. J. McCall, D. G. York, and P. Sonnentrucker, "Unusually Weak Diffuse Interstellar Bands toward HD 62542", *Astrophysical Journal*, 573, p. 670, 2002.
3. J. E. Gunn et. al., "The Sloan Digital Sky Survey Photometric Camera", *AJ*, 116, pp. 3040-3081, 1998.
4. Daniel J. Schroeder, "Optical Design of the ARC Echelle Spectrometer", *Instrumentation for Ground-Based Optical Astronomy, Present and Future*, Editor L. B. Robinson, The Ninth Santa Cruz Workshop in Astronomy and Astrophysics, pp. 39-46, Springer-Verlag, New York, 1988.
5. R. F. Loewenstein and D. G. York, "Instrument control and user interface for the ARC 3.5m observatory", *Instrumentation in Astronomy VI*, Editor David L. Crawford, SPIE Vol. 627, pp. 162-166, Tucson, 1986.
6. Julie A. Thorburn et al., manuscript in preparation.

## 10. ACKNOWLEDGEMENTS

We gratefully acknowledge the work of many people in making this a working facility instrument: Al Harper, Doug Duncan, Bob Pernic, Bob Hirsch, and Ellen LaRue, of the University of Chicago; Mark Klaene, Craig Loomis, Russet McMillan, Dave Woods, Karen Loomis, Jon Davis, Camron Hastings, Gretchen Van Doren, and Bruce Gillespie of the Apache Point Observatory; Daniel Schroeder (Beloit College), Sean Callahan (University of Arizona), Thomas McMahan (University of Arizona), Fred Mrozek (Recon Optical), and Paul Gettings (University of Utah). Financial support was provided by the Astrophysical Research Consortium and by the University of Chicago.